

Recyclable Mn(I) Catalysts for Base-Free Asymmetric Hydrogenation: Mechanistic, DFT and Catalytic Studies

Harikrishnan Jayaprakash,^{*[a]} Peter Coburger,^[a] Michael Wörle,^[a] Antonio Togni,^[a] and Hansjorg Grützmacher^[a]

Dedicated to Professor Christian Bruneau

Abstract: We report here a mechanistic, DFT and catalytic study on a series of Mn(I) complexes **1**, **2(a–d)**, **3**, **4**. The studies apprehended the requirements for Mn(I) complexes to be active in both asymmetric direct (AH) and transfer hydrogenations (ATH). The investigations disclosed 6 vital factors accelerating the formation of a resting species, which plays a significant role in lowering the activities of the Mn(I) complex **1** in ATH and AH, respectively. In addition, we also

report here a base free Mn(I) catalyzed ATH of aryl alkyl ketones with high enantioselectivity (up to 98% ee) and improved activity. More significantly, a novel and simple single-step process for recycling the resting species from the catalytic leftover has been discovered. Notably, the studies provide evidence for the existence of two different temperature dependent mechanisms for AH and ATH, in contrast to previous studies on related systems.

Introduction

Enantioselective hydrogenation of polar double bonds with transition-metal catalysts have seen broad scope of application after the discovery of Noyori's catalyst (Scheme 1, **A**).^[1] Despite showing excellent efficiency,^[2,3] due to their high cost and low earth-abundance, noble metal catalysts are being currently replaced to a significant extent by first-row metal catalysts for asymmetric hydrogenation.^[4–11] The last decade has witnessed the development of several Fe(II) catalysts for hydrogenation, some of which showed both good activity and excellent enantioselectivities (Scheme, **B**, **C**).^[12–17]

In contrast, Mn(I) catalysts have been studied for such transformations only since 2016,^[18,19] though they are cheap, less toxic and comparably more air stable than Fe(II) catalysts. Mn(I)-catalyzed asymmetric transfer hydrogenation (ATH)^[20–24] of ketones are less explored compared to asymmetric direct hydrogenation (AH).^[25–32] Moreover, the observed enantioselectivities for ATH with well-defined Mn(I) complexes such as **D**, **E** and **F** (Scheme, 20%–85% ee)^[21,23,24] and also other Mn(I) catalytic systems (1%–90 ee%)^[20,22] are significantly lower when

compared to those for AH (7%–99% ee).^[25,27–33] With the exception of Clarke's complex (**F**), Mn(I) catalysts are reported to be active either in AH or in ATH, but not necessarily in both.

Furthermore, the observed activities of Mn(I) asymmetric hydrogenation catalysts are lower (cat. loading of 0.5–1 mol%) when compared to iron or ruthenium catalysts (as low as 1 ppm, Scheme 1).

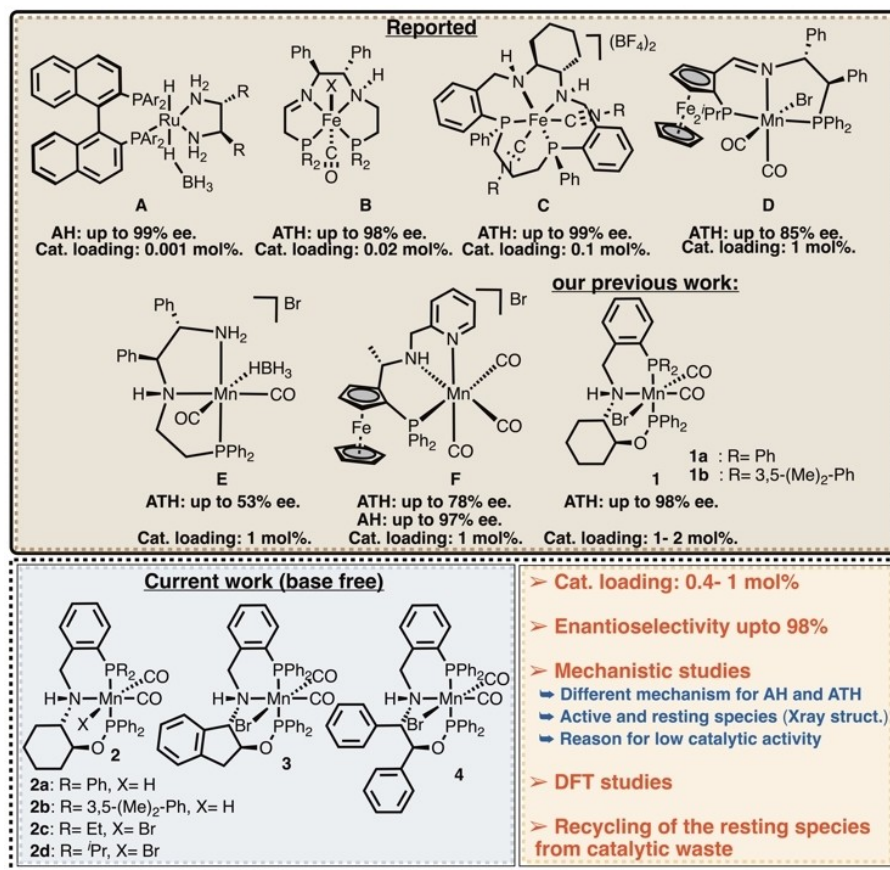
As Mn(I)-catalysts for asymmetric hydrogenation are studied only since 2016, their mechanistic features are less understood. Milstein's group has provided crucial evidence for the existence of two Mn(I) intermediates in AH^[34] and Lan's group has given significant insight on the ligand's role for the activity of Mn(I) complexes.^[35] Despite these contributions, several uncertainties, such as the reasons for the low activity of Mn(I) hydrogenation catalysts, requirement for Mn(I) complexes to be active in both AH/ATH, and a simple methodology to recycle the resting species from catalytic leftover are still left unanswered. Due to these reasons, an efficient Mn(I) catalysts for asymmetric hydrogenations with greater practical significance is still to be developed. Therefore, a deeper mechanistic insight is highly significant.

We report here mechanistic, DFT and catalytic studies on a series of Mn(I) complexes **2(a–d)**, **3**, **4**. This study reveals the crucial requirements for any Mn(I) complexes to be active in both asymmetric direct (AH) and transfer hydrogenation (ATH) and the reasons for the commonly observed trend in the activities of Mn(I) complexes in AH and ATH. In addition, we have also developed Mn(I) catalysts (**2a–2c**) for base-free ATH of aryl alkyl ketones with high enantioselectivity (up to 98% ee) and activity (as low as 0.4 mol% catalytic loading). More significantly, a single-step process to recycle the catalytic leftover (**5d/5d'**) has been discovered. Notably, the evidence for the existence of two different mechanisms for AH and ATH

[a] H. Jayaprakash, Dr. P. Coburger, Dr. M. Wörle, Prof. A. Togni, Prof. Dr. H. Grützmacher
Department of Chemistry and Applied Biosciences
Swiss Federal Institute of Technology (ETH) Zürich
8093 Zürich (Switzerland)
E-mail: hari@inorg.chem.ethz.ch

Supporting information for this article is available on the WWW under <https://doi.org/10.1002/chem.202201522>

© 2022 The Authors. Chemistry - A European Journal published by Wiley-VCH GmbH. This is an open access article under the terms of the Creative Commons Attribution Non-Commercial NoDerivs License, which permits use and distribution in any medium, provided the original work is properly cited, the use is non-commercial and no modifications or adaptations are made.



Scheme 1. Comparison of reported catalysts with new Mn(I) catalysts (2,3,4) for the asymmetric hydrogenation of ketones.

that are highly temperature dependent are in contrast with previously reported studies on related Mn(I) catalytic systems.

Results and Discussion

With the recently reported manganese complexes (**1**), the aryl-alkyl ketones were reduced with good enantioselectivity but with low yields.^[23] Moreover, complexes **1** suffer from a detrimental effect on increasing the temperature from 40 °C to 80 °C (Figure 1). Hence, to gain better insight on the reason for lower activity, mechanistic studies were necessary.

Initially, complex **1a** led to the formation of Mn(I) amido species **5a** and Mn(I) *tert*-butoxo species **5e** (Scheme 2), upon treatment with KO^tBu in benzene (1 equiv.) at –20 °C, which were identified by their distinctive ³¹P NMR chemical shifts (Scheme 2).^{[27],[33]} The *tert*-butoxo species **5e** gradually leads to Mn(I) amido species **5a** in an hour which eventually forms metalla-aziridine complex **5d**. It is to be noted that only **5d** and trace of **5a** (less than 10%) was observed upon treating complex **1a** with KO^tBu in benzene (1 equiv.) at 40 °C. Therefore, *iso*-propoxo species **5b** is expected to be a transition state during the reaction at 40 °C.

Furthermore, under similar conditions (**5a**, KO^tBu (1 equiv.), benzene), in the presence of ⁱPrOH (5 equiv.) at 40 °C, amido

species **5a**, hydride complex **2a** and unreacted complex **1a** was observed at 1 h reaction time. However, only hydride complex **2a** was found in the reaction mixture at 3 h which gradually lead to the formation of metalla-aziridine complex **5d** upon further reaction. However, under the previously reported catalytic condition (C: **1a**, 2 mol%; KO^tBu, 4 mol%; 40 °C; 2 M in ⁱPrOH) in the presence of acetophenone, though **1a**, **5a** and **5c** were observed during the course of the reaction (1–3 h), only **5c** and traces of **5d** were observed after 4 h (Scheme 2).

This illustrates that **1a** leads to the formation of amido species **5a** in the presence of base. Consecutively, **5a** being unstable leads to the formation of comparably highly unstable Mn(I) *iso*-propoxo species **5b** (transition state), which eventually undergoes β-H elimination to form the corresponding Mn(I) hydride **2a** via elimination of acetone (Scheme 2). **2a** then performs hydride attack on the carbonyl carbon of the incoming acetophenone leading to the formation of **5c**, identified by its distinctive ³¹P chemical shifts (Scheme 2). Finally, **5a** is regenerated via extrusion of enantioenriched alcohol from **5c** (Scheme 2). All intermediates (**5a**, **5b**, **2a**, **5c**) formed were finally transformed to the metalla-aziridine species **5d** during the time of the reaction (Scheme 2). Complexes **2a** (CCDC 2159791) and **5d** (CCDC 2159715) were isolated and characterized by X-ray crystallography and NMR spectroscopy. The intermediates **5a**, **5b** and **5c** were characterized by ³¹P

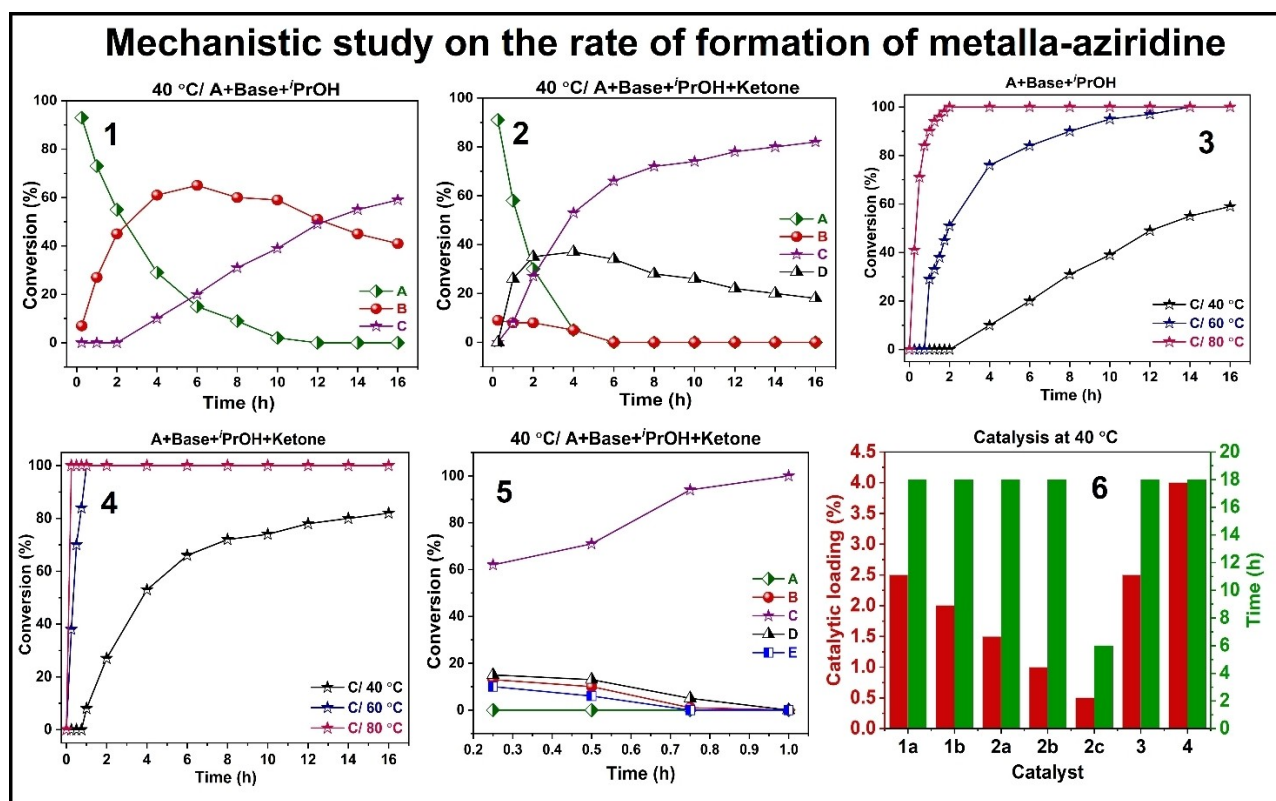


Figure 1. Mechanistic study on the rate of formation of metalla-aziridine. (1) Formation of the intermediates in the condition X. (2) formation of the intermediates in the condition Y. (3) Formation of metalla-aziridine 5d in the condition X at different temperatures. (4) Rate of formation of the metalla-aziridine from 2c in the condition Y. 5) Time required for the completion of catalysis with different catalyst. (A=Mn(I) catalyst 1a (2c in the case of graph 5), B=Mn(I) hydride 2a, C = metalla-aziridine 5d, D=Mn(I) alkoxide 5c), Catalytic conditions X: catalytic loading: 2 mol%, 4 mol% KO^tBu; Y: catalytic loading: 2 mol%, 4 mol% KO^tBu, acetophenone.

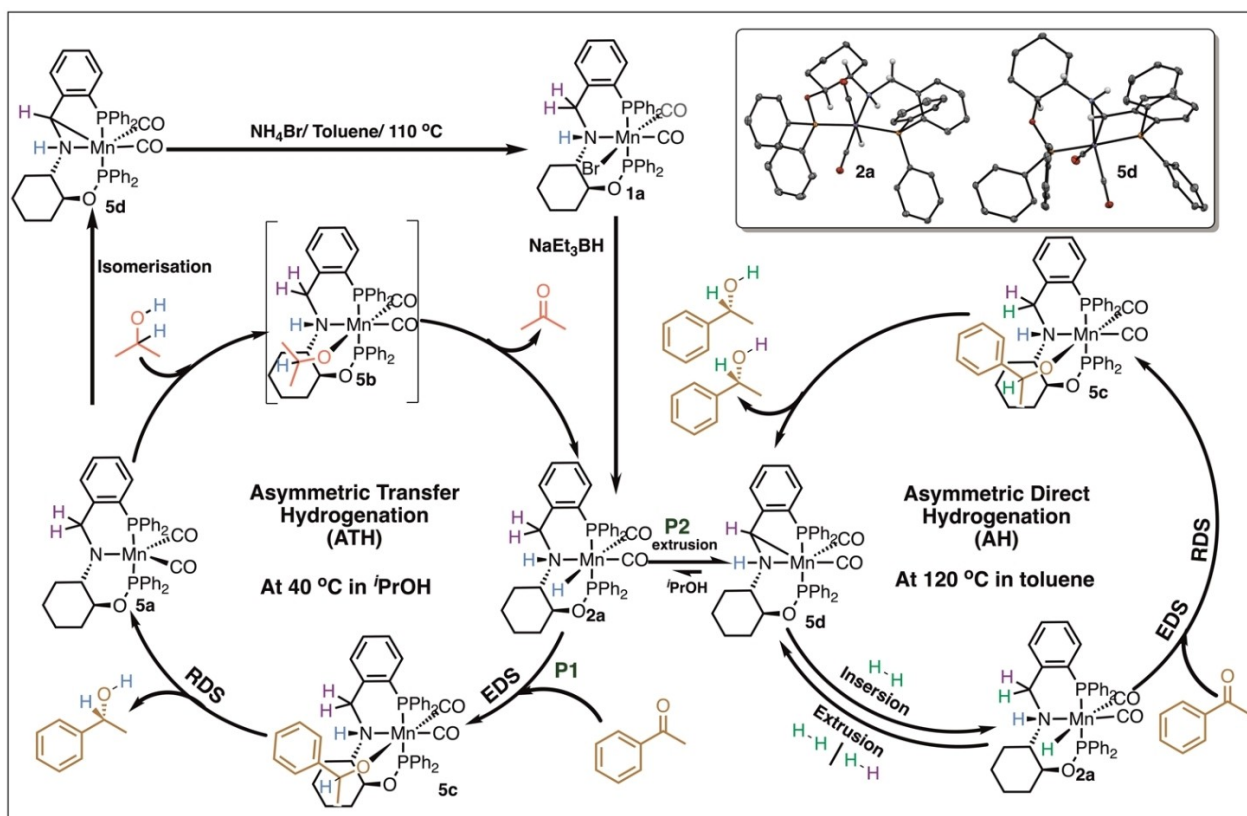
NMR chemical shifts at -20°C , 40°C (5a); -20°C (5b) and 40°C (5c), respectively (see Supporting Information). This leads us to the conclusion that the stability (thermodynamic stability, see DFT for further details) of the intermediates follows the order: $5b < 5a < 2a < 5c < 5d$. Since 5c was the only active species left after 10 h at 40°C in the catalysis (by ^{31}P NMR), formation of 5a from 5c was identified to be the rate determining step (RDS) in the catalytic cycle.

As 5d is the most stable and resting species in the catalytic cycle, a mechanistic study was conducted to follow the rate of formation of metalla-aziridine intermediate 5d during the course of the catalytic cycle. The formation of 5d at low temperature is in contradiction with the results obtained by Milstein (see below).^[34] The mechanistic studies revealed, as to be expected, that the rate of formation of 5d increases with temperature (Figure 1, graph 3). After 18 h (reaction time), only 5d was observed in the reaction mixture. The disability of 5d to convert acetophenone to its corresponding chiral alcohol by ATH, confirms that 5d is indeed the resting species in the catalytic cycle (see Supporting Information). This explains the reason for the detrimental effect on the activity of the previously reported Mn(I) complexes (1) at higher temperatures.^[23] These mechanistic studies also shed light on the fact that the rate of formation of 5d is significantly higher

under catalytic conditions than in the absence of acetophenone (Figure 1, graph 1 and 2). This indicates that there is more than one pathway for the formation of 5d within the catalytic cycle. Therefore, in order to obtain a better insight in the mode of formation of 5d, we focused on the synthesis of catalytically active hydride complex 2a and tested its tendency towards the formation of 5d in the absence of base.

The manganese hydride 2a was obtained as a mixture of two isomers (*syn:anti* = 4:3)^[36] by reacting 1a with NaEt₃BH at r.t. in benzene, of which only *syn*-2a was found to be catalytically active (see Supporting Information, scheme 2). To our surprise, despite heating 2a at 40°C for 24 h (under base-free conditions), 5d was not formed. Interestingly, 5c was still formed from 2a under catalytic conditions (1 mol% 2a, acetophenone, *i*PrOH, 40°C), though extrusion of hydrogen from 2a requires higher temperatures, typically 60°C (see Supporting Information). This led us to conclude that isomerization of the amido species 5a and extrusion of hydrogen from 2a are the two active pathways for the formation of 5d during the catalytic cycle and both pathways get accelerated in the presence of base (see figure 1, Supporting Information).

This instigated us to deploy the manganese hydride 2a directly for ATH of acetophenone in order to eliminate the presence of base, so as to reduce the formation of 5d (via base



Scheme 3. Mechanistic comparison between ATH and AH at different temperatures under base free conditions.

calculations corroborate that the hydricity of **2a** is lowered by $3.5 \text{ kcal}\cdot\text{mol}^{-1}$ when compared to that of **2c** (see Supporting Information).

As expected **2c** displayed an improved activity (0.4 mol% cat. loading) in ATH in comparison with **2a** (4 mol% cat. loading)) by approximately four times. An attempt to further increase the electron density by introducing the bis-isopropyl phosphino group (**2d**) instead of PEt_2 (**2c**) failed as the catalyst (**2d**) was found to be inactive. A possible explanation for this observation is that, as we increase the number of methyl substituent on the α -carbon of the phosphine, the steric bulk (cone angle)^[39] increases significantly to such an extent that the incoming aryl-alkyl ketone (acetophenone) fails to productively interact with the corresponding Mn(I) hydride complex of **2d** to undergo ATH. Since we were also suspecting that the acidity of the benzylic carbon next to the coordinated nitrogen atom of the ligand plays an important role (deprotonation of the benzylic proton is inevitable for the formation of **5d**), our focus was then centered on determining the consequence of change in the acidity of the benzylic proton.

Therefore, we have deployed **4** in ATH of acetophenone under standard catalytic conditions (**4**, 2 mol%; KO^tBu , 4 mol%; 40°C ; $i\text{PrOH}$, 2 M) with the rationale that a larger number of benzylic carbon atoms with acidic protons will enhance the possibility of formation of the corresponding metalla-aziridine, leading to a comparably less active catalyst. As expected, the

activity of **4** was approximately half that of its parent complex **2a** (see Supporting Information). This indicates that the acidity and the number of benzylic protons next to the coordinated nitrogen atom of the ligand have an inverse effect on the activity of the manganese complex.

A comparison of X-ray data of **2a**, **5d**, clearly shows that in **2a** the ring incorporating the benzylic carbon centre **5'** with its acidic protons resides in a strained six-membered metallacycle with a boat conformation and upon deprotonation forms a three-membered metalla-aziridine and an annulated five-membered metallacycle in a stable envelop shape (Figure 2).

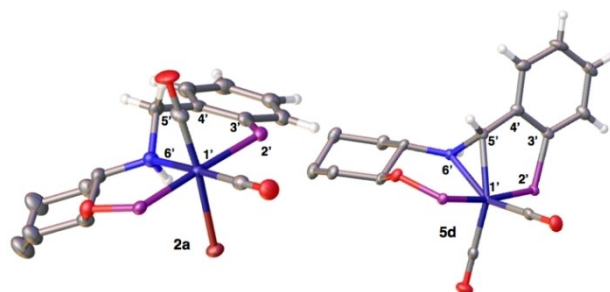


Figure 2. Comparison of the X-ray crystal structures of **2a** and **5d** (Phenyl rings on the phosphorous atoms (violet colour) and selected protons are deleted for better understanding).

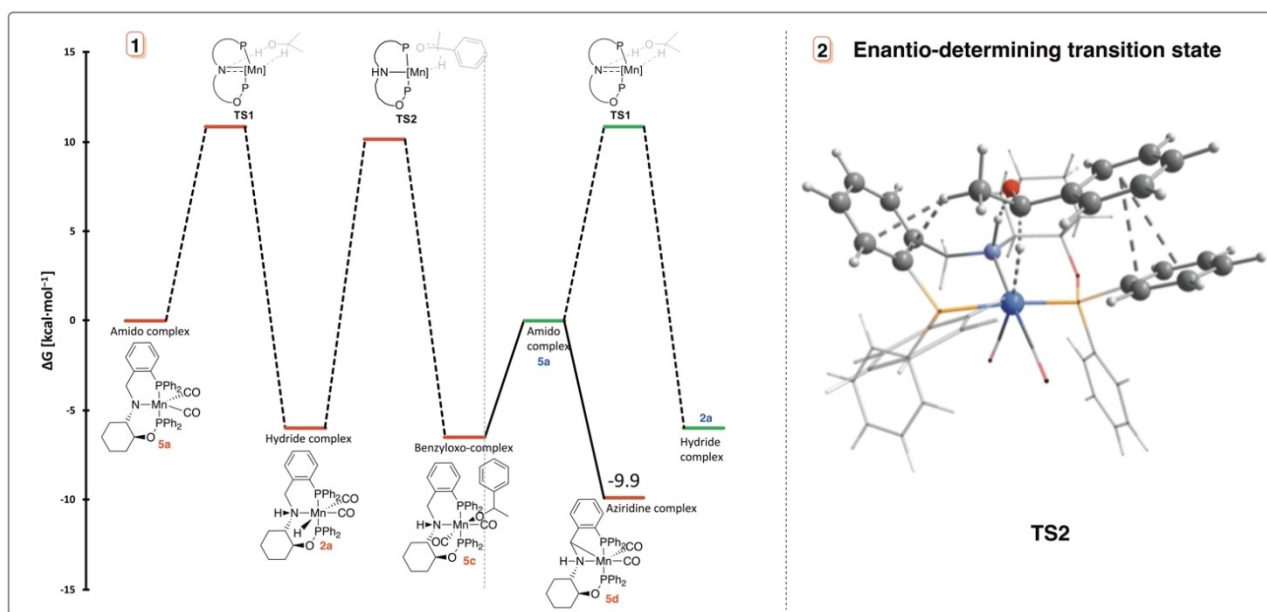


Figure 3. 1. The proposed reaction profile calculated by use of DFT (using the ORCA program package) for the hydrogenation of acetophenone catalysed by the manganese amido complex (1Mn) at RT in ⁱPrOH. 2. Interactions in the transition state (TS2) resulting in the enantioselectivity of the catalytic cycle.

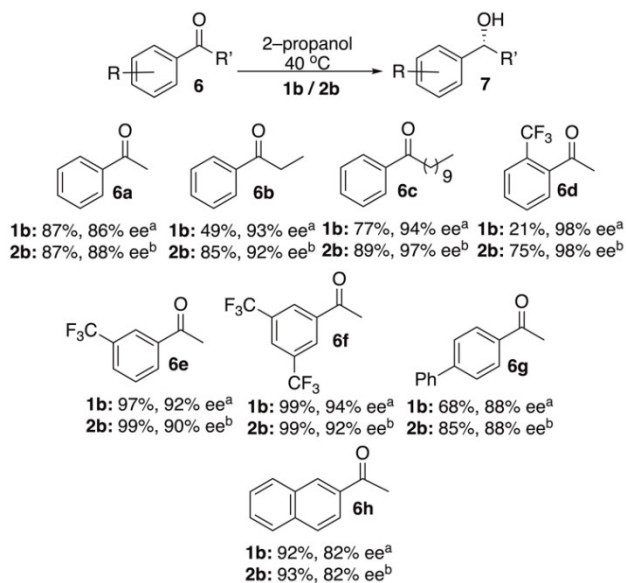
Our mechanistic studies indicate that the metalla-aziridine is the thermodynamically most stable intermediate (resting species) in the catalytic cycle and is responsible for lowering the activity of manganese complexes. A possible explanation for the tendency of Mn(I) catalysts to form the metalla-aziridine is its general tendency to prevail as an electron-rich (stable) Mn(I) complex with soft ligands. Since the σ -bonded benzylic ligand is less electronegative and softer when compared to the nitrogen atom of the amido species, **5d** is more electron-rich/stable than **5a**. This hypothesis is corroborated by the fact that the electron-rich Mn(I) complex **2c** is less prone towards metalla-aziridine formation (in the presence of ketone) and therefore displays an increased activity when compared to **1a**. Since the Mn(I) complexes are rather electrophilic, external factors such as base and temperature in conjunction with internal factors like number of benzylic carbon atoms next to the coordinated nitrogen, the number and acidity of the corresponding protons, ring size and steric strain of the metallacycle facilitate the formation of electron-rich, stable, and catalytically inactive Mn(I) metalla-aziridine.

In order to verify our mechanistic hypotheses on ATH, DFT studies were conducted. A possible mechanism in full agreement with the experimental findings could be modeled. Starting from **5a**, the metal hydride species **2a** is formed by a concerted dehydrogenation of isopropanol (TS1). This reaction is exergonic ($\Delta G = -6.0 \text{ kcal}\cdot\text{mol}^{-1}$) and proceeds via a low-lying transition state ($\Delta G = 10.8 \text{ kcal}\cdot\text{mol}^{-1}$). In the next step, the hydride is transferred to the α -carbon atom of acetophenone, resulting in the benzyl alkoxide species **5c**. This step is almost thermoneutral ($\Delta G = -6.0 \text{ kcal}\cdot\text{mol}^{-1}$) and proceeds via a total activation barrier of $16.1 \text{ kcal}\cdot\text{mol}^{-1}$. In addition to the RDS, DFT also elucidated the enantio-determining-step (EDS). In

this the activated complex at the transition state TS2 is stabilized by π - π stacking and CH_3 - π interactions (Figure 3). Finally, endergonic dissociation ($\Delta G = 6.5 \text{ kcal}\cdot\text{mol}^{-1}$) of benzyl alcohol from **5c** regenerates the active catalyst **5a**. In line with the experimental findings, the total activation barrier to reach TS1 from **5a**, and thus to begin the next catalytic cycle, is higher than to transfer a hydride to acetophenone ($17.3 \text{ kcal}\cdot\text{mol}^{-1}$ vs. $16.1 \text{ kcal}\cdot\text{mol}^{-1}$) and therefore corroborates the proposed mechanism and the previously observed order of stability of the intermediates ($5a < 5b < 2a < 5c < 5d$).

With the obtained knowledge on the behavior of the Mn(I) complexes (**1a–1b**, **2a–2d**, **3** and **4**), we then advanced to investigate a selected substrate scope with the best performing catalyst (**2b**), so as to further validate the acquired mechanistic and DFT insights and also to have a comparison with the previously reported Mn(I) complex **1b**. Hence, with the identified optimal reaction conditions C1 (**1b**, 2 mol%; KO^tBu, 4 mol% (1 M in THF); 40 °C; 0.2 M in ⁱPrOH; 18 h) and C2 (**2b**, 0.9 mol%; KO^tBu, 2 mol%; 40 °C; 0.2 M in ⁱPrOH; 24 h), ATH of aryl-alkyl ketones was performed (Schemes 3).

Aryl-alkyl ketones with various alkyl and aryl substituents were investigated for their reactivity with catalyst **1b/2b** (Scheme 4). As expected, **2b** has shown approximately doubled activity when compared to **1b** for ATH of aryl-alkyl ketones (this is consonant to the obtained mechanistic observations). In particular, with the reoptimized conditions C4 (Scheme 4), **2b** gives the trifluoromethyl-substituted alcohols **7e** and **7f** which are important synthons for fungicides^[40] and NK₁ antagonists^[41] in quantitative yields and with 90% and 92% ee, respectively. Notably, the same results were observed with **6e** and **6f** even with lower catalytic loading of 0.5 mol% when compared to previously reported 1 mol% catalytic loading with **1b** under



Scheme 4. Asymmetric transfer hydrogenation with catalyst **1b/2b**: isolated yields are given and ee values were determined by GC and HPLC, respectively. a. Optimized condition **C1** (catalytic loading: 2 mol%, 4 mol% KO^tBu, 40 °C, 18 h, 0.2 M). b. Optimized condition **C2** (catalytic loading: 0.9 mol%, 40 °C, 24 h, 0.2 M). c. reoptimized condition **C3** (catalytic loading: 1 mol%, 2 mol% KO^tBu, RT, 18 h, 0.2 M). d. reoptimized conditions **C4** (catalytic loading: 0.5 mol%, RT, 24 h, 0.2 M).

conditions **C3**. To the best of our knowledge, the obtained results are among the best when compared with other reported manganese complexes for ATH. It is to be also noted that sterically demanding ketones (cyclohexyl phenyl ketone, *tert*-butyl phenyl ketone) and dialkyl ketones were not reduced with **2b**. Further ketones were not tested for ATH as the pattern of observed enantioselectivity with **2b** were found to be corroborating with the previously reported complex **1b**.^[23]

More importantly, a unique strategy has been developed to recycled back **1a** from the resting species in the catalytic leftover. After the completion of the reaction, the solution was dried under vacuum and obtained residue was washed with hexane for 3–4 times (10 mL) to remove the unreacted ketone and enantioenriched alcohol from the reaction mixture. The leftover residue (only the resting species from the catalytic cycle: **5d**) when dried and upon treating with NH₄Br (2 equiv.) in toluene (2 M) at 110 °C, led to the recycling of **5d** to pre-catalyst **1a** (93% yield). Our studies have shown that the pre-catalyst **1a** could perform ATH with approximately same enantioselectivity ($\pm 2\%$) even upon recycling **5d** for three consecutive time. This makes **1/2** a more atom economic alternative with a potential practical relevance for ketone hydrogenation.

It was also found that treating **1a** with base in any polar/apolar aprotic solvent resulted exclusively in the formation of **5d**. This could be due to the lack of acid to protonate the highly reactive amido nitrogen coordinated to Mn(I). Due to the above observation, we expected **1a/2a** to be inactive in AH and indeed they were found to be so under various conditions (Table 2 and Supporting Information). However, both **1a** and

Table 2. Effect of electron density on ligand's donor atom and structural rigidity on the activity and enantioselectivity of the complexes. For ATH of ketones.

S.No.	Solvent [2 M]	Catalyst	Temperature [°C]	Yield [%]	ee [%]
1	X	1a	40	nd	nd
2	toluene	1a	80	nd	nd
3	toluene	1a	120	20	10
4	xylene	2a ^a	120	39	10
5	xylene	2a	130	46	6
6	xylene	2a	140	99	27
7	xylene	2b	110	52	10
8	xylene	2b	130	99	32
9	toluene	2c	90	54	44
10	toluene	2c	100	70	44
11	toluene	2c	110	99	50
12	xylene	5d	130	44	6
13	xylene	4	130	30	40

Reaction condition: Catalyst (2 mol%), KO^tBu (4 mol%), 18 h. [a] Catalyst (2 mol%), 18 h. X = toluene, MeOH, EtOH, THF, DMSO, benzene, xylene.

2a were found to be active at temperatures above 120 °C (up to 140 °C, in a closed reaction vessel) in toluene (see Supporting Information). This implies that the resting species (**5d**) present in solution (between r.t. and 120 °C), undergoes addition of H₂ at 120 °C. A possible explanation for this behavior is that **5d** attains the required activation threshold at 120 °C, leading to the cleavage of the σ -Mn(I)-benzylic bond and thereby promoting the activation of molecular hydrogen via insertion to form Mn(I) hydride complex (**2a**). Complex **2a** can then potentially undergo two different pathways. Firstly, H₂ is extruded to form **5d** (elimination of H₂ from **2a** occurs at temperatures between 40 °C and 60 °C). Secondly, **2a** immediately performs hydride attack on an incoming ketone. Subsequently, the formation of **5c** is achieved under the liberation of racemic alcohol and regeneration of **5d**. Since the extrusion of H₂ from **2a** is more favorable than

performing hydride attack on the incoming ketone at high temperature, formation of **5c** from **2a** is the RDS of AH. Moreover, RDS and EDS remain the same for AH, as the *re* and *si* selective hydride attack on the incoming ketone determines the enantioselectivity (Scheme 3). This finding suggests the existence of two different mechanisms for AH and ATH.

According to ³¹P NMR studies, at any given time two isomers of metalla-aziridine (**5d/5d'**) are observed at temperatures between 40 °C and 130 °C. The presence of two diastereoisomers at 130 °C is the primary reason for the observation of nearly racemic alcohols (6–10% ee) on AH of acetophenone with **1a/2a** (see Supporting Information). In order to corroborate the above-mentioned conjecture, **4** was employed in AH of acetophenone (principle: presence of a stereogenic benzylic carbon should promote chiral induction via metalla-aziridine resulting in the production of enantioenriched alcohols). According to our expectation, catalyst **4** led to an enhanced enantioselectivity of 40% in AH of acetophenone. This is in support of the argument that **5d** (resting species in ATH) is an active intermediate in AH and also demonstrates that the amido species **5a** is not involved in AH.

Finally, we wanted to assess the effect of the electron donating capacity of the ligand on the weakening of the Mn(I)-alkyl bond which should be reflected in the activity of **5d** in AH of acetophenone. As shown in Table 2, by introducing electron-donating groups at the phosphorus centre to give complexes **2a–2d**, the activity of the complexes as catalysts at 120 °C increases. Only **2d** is an exception because the presence of sterically demanding *tert*-butyl substituents in the phosphinyl group block the access to the Mn(I) centre. We assume that the electron donating capacity of the ligands significantly decreases the activation barrier for the cleavage of the Mn(I)-carbon bond of the corresponding metalla-aziridine. Consequently, Mn(I) complex **2c** endures AH with quantitative yields at much lower temperature (90 °C) when compared with **2a** (140 °C) and **2b** (120 °C, Table 2). This finding also matches the observations made with other Mn(I) complexes that have been reported to date, i.e., as the electron density on the Mn(I) centre increases, the temperature required to AH significantly decreases. These discoveries also agree with the observations made by Lan's group (ligand's role for the activity of the Mn(I) complexes)^[35] and explains the reason for the exceptional activity of Pidko's mixed donor Mn(I) pincer complex (catalytic loading down to 5 ppm).^[42]

In addition to the above observations, the mechanistic studies revealed that both isomers of metalla-aziridine (**5d/5d'**) gradually convert to one single isomer at 140 °C with different ³¹P NMR chemical shifts and coupling constants and therefore is expected to be **5d''**. Metalla-aziridines **5d** and **5d'** are diastereoisomers and display the absolute configuration *S* and *R*, respectively,^[43] at the benzylic carbon. Whereas metalla-aziridine **5d''** with '*S*' configuration is formed via stereospecific C–H activation at C₂ of the aminocyclohexanol and the corresponding carbanion is comparatively more σ-donating than the benzylic carbon. The metalla-aziridine may therefore be considered as an intermediate in the catalytic cycle, which exists in its two kinetically stable forms **5d/5d'** (Figure 4) and

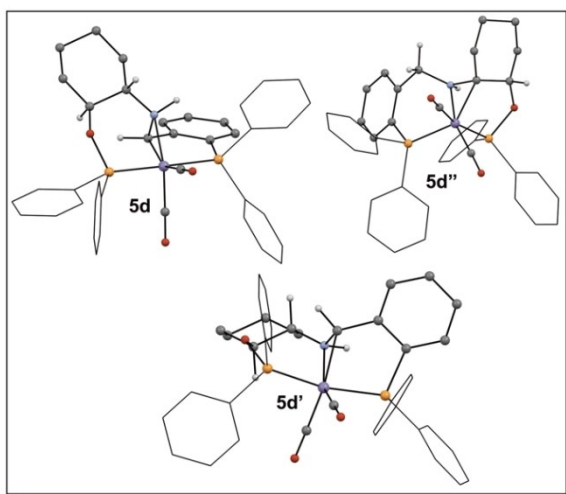


Figure 4. DFT optimised structures of three different Mn(I) aziridines (**5d/5d'** (kinetic intermediates) and **5d''** (thermodynamic intermediate)).

one thermodynamically stable form **5d''** (figure 4). Since there is only one single thermodynamically stable metalla-aziridine, **5d''** was tested for its efficiency in AH. As expected it showed enhanced enantioselectivity (27%). However, an attempt to increase the temperature in order to further enhance the enantioselectivity failed due to the decomposition of the complexes at temperatures above 150 °C.

The same trend of enhancement of enantioselectivity with increasing temperature was also observed with complexes **2b** and **2c**, which again indicates that only the metalla-aziridine is involved as intermediate in AH. The above findings (enhancement of enantioselectivity with both **4** and **5d''**, **5a** is not involved in AH) in combination with the observation from the mechanistic studies that the RDS and EDS steps for both ATH and AH are different, demonstrates that two different mechanistic pathways are operative for AH and ATH that are highly temperature dependent (Scheme 3). This discovery has also led to the clarification of a much-believed deception that both the Mn(I) hydride and Mn(I) aziridine intermediates are equally responsible/involved in AH and ATH of ketones.

Conclusion

A series of recyclable Mn(I) complexes (**2**) was developed and the requirements for them to be active in both asymmetric transfer (ATH) and direct hydrogenation (AH) were identified. Mechanistic studies on the previously reported manganese complex (**1**) have revealed that the metalla-aziridine (resting species, **5d/5d'**) formation plays a significant role in lowering and quenching the activities of the Mn(I) complexes **1** in ATH and AH, respectively. The mechanistic work also revealed that in addition to the (a) base, (b) temperature, (c) acidity of proton on the α-carbon to the coordinated nitrogen atom, (d) number of benzylic protons on the α-carbon, (e) steric strain of the metallacycle, and (f) ring size of the pincer complex are further important factors that facilitate the formation of metalla-aziridines, which are catalytically inactive in ATH. The DFT studies agree with the mechanistic studies and, moreover, revealed that *CH*-π interactions from the aryl rings on the ligand's phosphine atom and the π-π interaction from the aryl rings on the ligand's phosphinite atom with that of the incoming ketones play the key role in determining the enantioselectivity.

We also report here a group of new Mn(I) hydride complexes **2** for base-free ATH of aryl alkyl ketones which led to high enantioselectivity (up to 98% ee) and improved activity (up to fourfold) when compared to the previously reported derivative **1**. A simple methodology has been discovered to recycle the resting species from the catalytic leftover to **1**, making **1/2** an attractive alternative towards ketone reduction. In addition, the studies indicate the existence of different mechanism for ATH and AH that are highly temperature dependent. This investigation may thereby facilitate the future design of better Mn(I) catalysts with improved practical relevance.

Deposition Numbers 2159791 and 2159715 contain the supplementary crystallographic data for this paper. These data are provided free of charge by the joint Cambridge Crystallographic Data Centre and Fachinformationszentrum Karlsruhe Access Structures service.

Acknowledgements

We thank the Swiss National Science Foundation for financial support (Grant no. 200020-181966). We also thank Prof. Victor Mougél for providing GC and HPLC facilities. Open Access funding provided by Eidgenössische Technische Hochschule Zürich.

Conflict of Interest

The authors declare no conflict of interest.

Data Availability Statement

The data that support the findings of this study are available in the supplementary material of this article.

Keywords: asymmetric catalysis · DFT studies · hydrogenation · manganese-catalyzed · mechanistic studies

- [1] R. Noyori, T. Ohkuma, *Angew. Chem. Int. Ed.* **2001**, *40*, 40–73; *Angew. Chem.* **2001**, *113*, 40–75.
- [2] J. H. Xie, X. Y. Liu, J. B. Xie, L. X. Wang, Q. L. Zhou, *Angew. Chem. Int. Ed.* **2011**, *50*, 7329–7332; *Angew. Chem.* **2011**, *123*, 7467–7470.
- [3] W. Wu, S. Liu, M. Duan, X. Tan, C. Chen, Y. Xie, Y. Lan, X. Q. Dong, X. Zhang, *Org. Lett.* **2016**, *18*, 2938–2941.
- [4] S. Murugesan, K. Kirchner, *Dalton Trans.* **2016**, *45*, 416–439.
- [5] D. Benito-Garagorri, K. Kirchner, *Acc. Chem. Res.* **2008**, *41*, 201–213.
- [6] A. Mukherjee, D. Milstein, *ACS Catal.* **2018**, *8*, 11435–11469.
- [7] P. J. Chirik, *Acc. Chem. Res.* **2015**, *48*, 1687–1695.
- [8] K. Junge, V. Papa, M. Beller, *Chem. A Eur. J.* **2019**, *25*, 122–143.
- [9] W. Ai, R. Zhong, X. Liu, Q. Liu, *Chem. Rev.* **2019**, *119*, 2876–2953.
- [10] D. Wei, C. Darcel, *Chem. Rev.* **2019**, *119*, 2550–2610.
- [11] S. Chakraborty, H. Guan, *Dalton Trans.* **2010**, *39*, 7427–7436.
- [12] L. C. Misal Castro, H. Li, J. B. Sortais, C. Darcel, *Green Chem.* **2015**, *17*, 2283–2303.
- [13] B. A. F. Le Bailly, S. P. Thomas, *RSC Adv.* **2011**, *1*, 1435–1445.
- [14] I. Bauer, H. J. Knölker, *Chem. Rev.* **2015**, *115*, 3170–3387.
- [15] R. Bigler, R. Huber, A. Mezzetti, *Angew. Chem. Int. Ed.* **2015**, *54*, 5171–5174; *Angew. Chem.* **2015**, *127*, 1–5.
- [16] A. Casnati, M. Lanzi, G. Cera, *Molecules* **2020**, *25*, 3889.
- [17] W. Zuo, A. J. Lough, Y. F. Li, R. H. Morris, *Science* **2013**, *342*, 1080–1084; **2013**, 1080–1084.
- [18] B. Maji, M. K. Barman, *Synth.* **2017**, *49*, 3377–3393.
- [19] Y. Wang, M. Wang, Y. Li, Q. Liu, *Chem* **2021**, *7*, 1180–1223.
- [20] K. Azouzi, A. Bruneau-Voisine, L. Vendier, J. B. Sortais, S. Bastin, *Catal. Commun.* **2020**, *142*, 106040.
- [21] K. Z. Demmans, M. E. Olson, R. H. Morris, *Organometallics* **2018**, *37*, 4608–4618.
- [22] J. Schneekönig, K. Junge, M. Beller, *Synlett* **2019**, *30*, 503–507.
- [23] H. Jayaprakash, *Dalton Trans.* **2021**, *50*, 14115–14119.
- [24] A. Zirakzadeh, S. R. M. M. de Aguiar, B. Stöger, M. Widhalm, K. Kirchner, *ChemCatChem* **2017**, *9*, 1744–1748.
- [25] L. Zhang, Y. Tang, Z. Han, K. Ding, *Angew. Chem. Int. Ed.* **2019**, *58*, 4973–4977; *Angew. Chem.* **2019**, *131*, 5027–5031.
- [26] C. S. G. Seo, B. T. H. Tsui, M. V. Gradiski, S. A. M. Smith, R. H. Morris, *Catal. Sci. Technol.* **2021**, *11*, 3153–3163.
- [27] A. Passera, A. Mezzetti, *Adv. Synth. Catal.* **2019**, *361*, 4691–4706.
- [28] L. Zeng, H. Yang, M. Zhao, J. Wen, J. H. R. Tucker, X. Zhang, *ACS Catal.* **2020**, *10*, 13794–13799.
- [29] M. B. Widegren, M. L. Clarke, *Catal. Sci. Technol.* **2019**, *9*, 6047–6058.
- [30] M. B. Widegren, G. J. Harkness, A. M. Z. Slawin, D. B. Cordes, M. L. Clarke, *Angew. Chem. Int. Ed.* **2017**, *56*, 5825–5828; *Angew. Chem.* **2017**, *129*, 5919–5922.
- [31] M. Garbe, K. Junge, S. Walker, Z. Wei, H. Jiao, A. Spannenberg, S. Bachmann, M. Scalone, M. Beller, *Angew. Chem. Int. Ed.* **2017**, *56*, 11237–11241; *Angew. Chem.* **2017**, *129*, 11389–11393.
- [32] F. Ling, H. Hou, J. Chen, S. Nian, X. Yi, Z. Wang, Di. Song, W. Zhong, *Org. Lett.* **2019**, *21*, 3937–3941.
- [33] C. Liu, M. Wang, Y. Xu, Y. Li, Q. Liu, *Angew. Chem. Int. Ed.* **2022**, *61*, e20220281; *Angew. Chem.* **2022**, e202202814. (Accepted article).
- [34] S. Chakraborty, U. Gellrich, Y. Diskin-Posner, G. Leitus, L. Avram, D. Milstein, *Angew. Chem. Int. Ed.* **2017**, *56*, 4229–4233; *Angew. Chem.* **2017**, *129*, 4293–4297.
- [35] Y. Wang, L. Zhu, Z. Shao, G. Li, Y. Lan, Q. Liu, *J. Am. Chem. Soc.* **2019**, *141*, 17337–17349.
- [36] H. Li, D. Wei, A. Bruneau-Voisine, M. Ducamp, M. Henrion, T. Roisnel, V. Dorcet, C. Darcel, J. F. Carpentier, J. F. Soulé, J. B. Sortais, *Organometallics* **2018**, *37*, 1271–1279.
- [37] K. M. Waldie, A. L. Ostericher, M. H. Reineke, A. F. Sasayama, C. P. Kubiak, *ACS Catal.* **2018**, *8*, 1313–1324.
- [38] E. S. Wiedner, M. B. Chambers, C. L. Pitman, R. M. Bullock, A. J. M. Miller, A. M. Appel, *Chem. Rev.* **2016**, *116*, 8655–8692.
- [39] J. Jover, J. Cirera, *Dalton Trans.* **2019**, *48*, 15036–15048.
- [40] K. Tanaka, M. Katsurada, F. Ohno, Y. Shiga, M. Oda, M. Miyagi, J. Takehara, K. Okano, *J. Org. Chem.* **2000**, *65*, 432–437.
- [41] K. M. J. Brands, J. F. Payack, J. D. Rosen, T. D. Nelson, A. Candelario, M. A. Huffman, M. M. Zhao, J. Li, B. Craig, Z. J. Song, D. M. Tschäen, K. Hansen, P. N. Devine, P. J. Pye, K. Rossen, P. G. Dormer, R. A. Reamer, C. J. Welch, D. J. Mathre, N. N. Tsou, J. M. McNamara, P. J. Reider, *J. Am. Chem. Soc.* **2003**, *125*, 2129–2135.
- [42] W. Yang, I. Y. Chernyshov, R. K. A. van Schendel, M. Weber, C. Müller, G. A. Filonenko, E. A. Pidko, *Nat. Commun.* **2021**, *12*, 1–8.
- [43] M. J. Sgro, D. W. Stephan, *Dalton Trans.* **2012**, *41*, 6791–6802.

Manuscript received: May 17, 2022

Accepted manuscript online: June 2, 2022

Version of record online: July 4, 2022